

1 Autumn – winter minimum temperature changes in the 2 southern Sikhote-Alin mountain range of northeast Asia since 3 1529 AD

4 Olga N. Ukhvatkina, Alexander M. Omelko, Alexander A. Zhmerenetsky, Tatyana Y. Petrenko.

5
6 Federal Scientific center of the East Asia terrestrial biodiversity Far Eastern Branch of Russian
7 Academy of Sciences, Vladivostok 690022 RUSSIA

8
9 *Correspondence to:* Olga Ukhvatkina (ukhvatkina@gmail.com)

10
11 **Abstract.** The aim of our research was to reconstruct climatic parameters (for the first time for the Sikhote-Alin
12 mountain range) and to compare them with global climate fluctuations. As a result, we have found that one of the
13 most important limiting factors for the study area is the minimum temperatures of the previous autumn-winter
14 season (August-December), and this finding perfectly conforms to that in other territories. We reconstructed the
15 previous August-December minimum temperature for 485 years, from 1529 to 2014. We found twelve cold periods
16 (1538-1543, 1549-1554, 1643-1649, 1659-1667, 1675-1689, 1722-1735, 1791-1803, 1807-1818, 1822-1827, 1836-
17 1852, 1868-1887, 1911-1925) and seven warm periods (1561-1584, 1603-1607, 1614-1618, 1738-1743, 1756-1759,
18 1776-1781, 1944-2014). These periods correlate well with reconstructed data for the Northern Hemisphere and the
19 neighboring territories of China and Japan. Our reconstruction has 2-4, 9-11, 48 and 189-year periods, which are in
20 line with high-frequency fluctuations in ENSO, the short-term solar cycle, PDO fluctuations and the de-Vier quazi-
21 200 solar activity cycle, respectively. We have confirmed the climatic response to solar activity, which corresponds
22 to cold periods during the solar minimum. These comparisons show that our climatic reconstruction based on tree-
23 ring chronology for this area may potentially provide a proxy record for long-term, large-scale past temperature
24 patterns for northeast Asia. The reconstruction reflects the global traits and local variations in the climatic processes
25 of the southern territory of the Russian Far East for more than the past 450 years.

26 1 Introduction

27 Global climate change is the main challenge for human life and natural systems, which is why we should clearly
28 understand climatic changes and their mechanisms. A retrospective review of climatic events is necessary for
29 understanding the climatic conditions from a long-term perspective. At the same time, instrumental climate
30 observations rarely cover more than a 100-year period and are often restricted to 50-70 years. This restriction forces
31 the researchers to continuously find new ways and methods to reconstruct climatic fluctuations. Dendrochronology
32 has been widely applied in climatic reconstruction for local territories and at the global scale for both climatic
33 reconstructions of the past few centuries and paleoclimatic reconstructions because it is rather precise, extensively
34 used and a replicable instrument (Corona et al.; Popp and Bouriaud, 2014; Kress et al., 2014; Lyu et al., 2016).
35 A great number of studies have focused on climatic change reconstruction for the northeastern parts of China based
36 on *P. koraiensis* radial growth studies (e.g., Zhu et al., 2009; Wang et al., 2013; Wang et al., 2016; Zhu et al., 2015;
37 Lyu et al. 2016). Climatic parameters were reconstructed for the whole Northern Hemisphere (Wilson et al., 2016),
38 China (Ge et al., 2016), and temperature characteristics were reconstructed for northeastern Asia (Ohshima et al.,
39 2013). Despite this, there are very few studies of Russian Far East climate (e.g., Willes et al., 2014; Jacoby et al.,
40 2004; Shan et al., 2015); moreover, there is an absence of dendrochronological studies for the continental part of
41 Russian Far East. Meanwhile, most of species present in northeastern China, the Korean peninsula and Japan grow in

42 this region. In addition, the distribution areas of these trees often end in the south of the Russian Far East, which
43 increases the climatic sensitivity of plants. Additionally, some parts of the forests in the Russian Far Eastern have not
44 been subjected to human activity for the last 2000-4000 years. This makes it possible to forests extend the studied
45 timespan. In addition, the southern territory of the Russian Far East is sensitive to global climatic changes as it is
46 under the influence of cold air flow from northeastern Asia during the winter and summer monsoons. All of the factors
47 listed above create favorable conditions for dendroclimatic studies.

48 It is well-known that warming of the climate is correlated with intensive solar activity (e.g., the Medieval Warm
49 Period), while decreases in temperature occurs during periods of low solar activity (e.g., the Little Ice Age; Lean and
50 Rind, 1999; Bond et al., 2001). According to findings from an area of China neighboring the territory studied here,
51 the registered warming has been significantly affected by global warming since the 20th century (Ding and Dai, 1994;
52 Wang et al., 2004; Zhao et al., 2009), which is often indicated by a faster rise in night or minimum temperatures (Karl
53 et al., 1993; Ren and Zhai, 1998; Tang et al., 2005). To better understand and evaluate future temperature change
54 trends, we should study the long-term history of climatic changes.

55 However, using tree-ring series for northeastern Asia (particularly temperature) is rather complicated due to the unique
56 hydrothermal conditions of the region. Most reconstructions cover periods of less than 250 years (e.g., Shao and Wu,
57 1997; Zhu et al., 2009; Wang et al., 2012; Li and Wang, 2013; Yin et al., 2009; Zhu et al., 2015), except for a few
58 with periods up to 400 years (Lyu et al., 2016; Wiles et al., 2014). The short period of reconstructions is the reason
59 why such reconstructions cannot capture low-frequency climate variations.

60 The warming of the climate (particularly minimum temperature increase) is registered across the whole territory of
61 northeastern Asia (Lyu et al., 2016). In the Russian Far-East, such warming has been recorded for more than 40 past
62 years (Kozhevnikova, 2009). However, the lack of detailed climatic reconstructions for the last few centuries makes
63 it difficult to capture long-period climatic events for this territory and interpret the temperature conditions for the last
64 500-1000 years.

65 Therefore, the main objectives of this study were (1) to develop the first three-ring-width chronology for the southern
66 part of the Russian Far East; (2) to analyze the regime of temperature variation over the past centuries in the southern
67 part of the Russian Far East; (3) to identify the recent warming amplitude in context of long-term changes and to
68 analyze the periodicity of climatic events and their driving forces. Our new minimum temperature record supplements
69 the existing data for northeast Asia and provides new evidence of past climate variability. There is the potential to
70 better understand future climatic trajectories from these data in northeast Asia.

72 **2 Materials and methods**

73 **2.1 Study area**

74 We studied the western macroslope of the southern part of the Sikhote-Alin mountain range (Southeastern Russia) at
75 the Verkhneussuriysky Research Station of the Federal Scientific Center of the East Asia terrestrial biodiversity Far
76 East Branch of the Russian Academy of Sciences (4400 ha; N 44°01'35.3'', E 134°12'59.8'', Fig. 1).

77 The territory is characterized by a monsoon climate with relatively long, cold winters and warm, rainy summers. The
78 average annual air temperature is 0.9 °C; January is the coldest month (−32 °C average temperature), and July is the
79 warmest month (27 °C average temperature). The average annual precipitation is 832 mm (Kozhevnikova, 2009).
80 Southerly and southeasterly winds predominate during the spring and summer, while northerly and northwesterly
81 winds predominate in autumn and winter. The terrain includes mountain slopes with an average angle of ~ 20°, and
82 the study area is characterized by brown mountain forest soils (Ivanov, 1964) (Fig. 2).

83 Mixed forests with Korean pine (*Pinus koraeinsis* Siebold et Zucc.) are the main vegetation type in the study area,
84 and they form an altitudinal belt up to 800 m above sea level. These trees are gradually replaced by coniferous fir-
85 spruce forests at high altitudes (Kolesnikov, 1956). Korean pine-broadleaved forests are formed by up to 30 tree
86 species, with *Abies nephrolepis* (Trautv.) Maxim, *Betula costata* (Trautv.) Regel., *Picea jezoensis* (Siebold et Zucc.)
87 Carr., *P. koraeinsis* and *Tilia amurensis* Rupr. being dominant.

88 Korean pine-broadleaved forests are the main forest vegetation type in the Sikhote-Alin mountain range in the
89 southern part of the Russian Far East. This area is the northeastern limit of the range of Korean pine-broadleaved
90 forests, which are also found in northeastern China (the central part of the range), on the Korean peninsula, and in
91 Japan. The Sikhote-Alin mountain range is one of the few places where significant areas of old-growth Korean pine-
92 broadleaved forest remain. In the absence of volcanic activity, which is a source of strong natural disturbances in the
93 central part of the range (Liu, 1997; Ishikava, 1999; Dai et al., 2011), wind is the primary disturbance factor on this
94 territory. Wind causes a wide range of disturbance events, from individual treefalls to large blowdowns (Dai et al.,
95 2011).

96 Approximately 60% of the Research Station area had been subjected to selective clear-cutting before the station was
97 established in 1972. The remaining 40% of its area has never been clear-cut and is covered by unique old-growth
98 forest.

99 2.2 Tree-ring chronology development

100 Our study is based on data collected in a 10.5-ha permanent plot (Omelko and Ukhvatkina, 2012; Omelko et al., 2016),
101 which was located in the middle portion of a west-facing slope with an angle of 22° at a gradient altitude 750-950 m
102 above sea level. The forest in the plot was a late-successional stand belonging to the middle type of Korean pine-
103 broadleaved forests at the upper bound of the distribution of Korean pine, where it forms mixed stands of Korean
104 pine-spruce and spruce-broadleaved forests (Kolesnikov, 1956).

105 One core per undamaged old-growth mature tree (25 cores from 25 trees) and one sample from dead trees (20 samples)
106 were extracted from *P. koraiensis* trees in the sample plots from the trunks at breast height. In the laboratory, all tree-
107 ring samples were mounted, dried and progressively sanded to a fine polish until individual tracheids within annual
108 rings were visible under an anatomical microscope according to standard dendrochronological procedures (Fritts,
109 1976; Cook and Kairiukstis, 1990). Preliminary calendar years were assigned to each growth ring, and possible errors
110 in measurement due to false or locally absent rings were identified using the Skeleton-plot cross-dating method
111 (Stokes and Smiley, 1968). The cores were measured using the semi-automatic Velmex measuring system (Velmex,
112 Inc., Bloomfield, NY, USA) with a precision of 0.01 mm. Then, the COFECHA program was used to check the
113 accuracy of the cross-dated measurements (Holmes, 1983). To mitigate the potential trend distortion problem in
114 traditionally detrended chronology (Melvin and Briffa, 2008; Anchukaitis et al., 2013), we used a signal-free method
115 (Melvin and Briffa, 2008) to detrend the tree-ring series using the RCSigFree program (<http://www.ldeo.columbia.edu/tree-ring-laboratory/resources/software>).

117 Age-related trends were removed from the raw tree-ring series using an age-dependent spline smoothing method. The
118 ratio method was used to calculate tree-ring indices, and the age-dependent spline was selected to stabilize the variance
119 caused by core numbers. Finally, the stabilized signal-free chronology was used for the subsequent analysis (Fig. 3).
120 The mean correlations between trees (*Rbt*), mean sensitivity (MS) and expressed population signal (EPS) were
121 calculated to evaluate the quality of the chronology (Fritts, 1976). *Rbt* reflects the high-frequency variance, and MS
122 describes the mean percentage change from each measured annual ring value to the next (Fritts, 1976; Cook and
123 Kairiukstis, 1990). EPS indicates the extent to which the sample size is representative of a theoretical population with

124 an infinite number of individuals. A level of 0.85 in the EPS is considered to indicate a chronology of satisfactory
125 quality (Wigley *et al.*, 1984). The statistical characteristics of the chronology are listed in Table 1.
126 The full length of the chronology spans (VUS chronology) from 1451 to 2015. A generally acceptable threshold of
127 the EPS was consistently greater than 0.85 from AD 1602 to 2015 (9 trees; Fig. 3b), which affirmed that this is a
128 reliable period. However, although the EPS value from AD 1529 to 1602 was less than 0.85, it matches a minimum
129 sample depth of 4 trees in this segment (EPS>0.75). It is very important to extend the tree-ring chronology as much
130 as possible because there are only a few long climate reconstructions in this area. Therefore, we retained the part from
131 1529 to 1602 in the reconstruction.

132 2.3 Climate data and statistical methods

133 Monthly precipitation, monthly mean and minimum temperature data were obtained from the Chuguevka
134 meteorological station (44.151462 N, 133.869530 E) and the meteorological post at the Verkhneussuriisky research
135 station of the Federal Scientific Center of the East Asia terrestrial biodiversity FEB RAS (Meteostation 7 – MP7) as
136 well. The periods of monthly data available from the Chuguevka and Verkhneussuriisky stations are 1936-2004 and
137 1969-2004, respectively (1971-2003 for minimum temperature data from the Chuguevka).

138 To demonstrate that our reconstruction representative and reflect temperature variations, we conducted spatial
139 correlation between our temperature reconstruction and gridded temperature dataset of the Climate Research Unit
140 (CRU TS4.00) for the period 1960-2003, by using the Royal Netherlands Meteorological Institute climate explorer
141 (<http://climexp.knmi.nl>).

142

143 2.4 Statistical analyses

144 A correlation analysis was used to evaluate the relationships between the ring-width index and observed monthly
145 climate records from the previous June to the current September. To identify the climate-growth relationships of
146 Korean pine in the southern Sikhote-Alin mountain range, a Pearson's correlation was performed between climate
147 variables and tree-width index. We used a traditional split-period calibration/verification method to explore the
148 temporal stability and reliability of the reconstruction model (Fritts, 1976; Cook and Kairiukstis, 1990). The Pearson's
149 correlation coefficient (r), R-squared (R^2), the reduction of the error (RE) the coefficient of efficiency (CE), and the
150 product means test (PMT) were used to verify the results. Analyses were carried out in R using the treeclim package
151 (Zang and Biondi, 2015) and STATISTICA software (StatSoft®).

152 3 Results

153 3.1 Climate-radial growth relationship

154 Relationships between the VUS chronology and monthly climate data are shown in Fig 4. To reveal the correlation
155 between climatic parameters and radial growth change of *P. koraiensis*, we had three data sets: the first-time series
156 had a length of 68 years (1936-2004, Chuguevka), the second had a length of 34 years (1966-2000, MP7), and the
157 third had a length of 33 years (1971-2003, Chuguevka, minimum temperature). To select the appropriate parameters,
158 we analyzed all datasets. As a result, we revealed a reliable but slight positive correlation between *P. koraiensis* growth
159 and precipitation in May and June of the current year and September of the previous year in the territory of Chuguevka
160 village (Fig. 4a). There is also a slight positive correlation with precipitation in September of the previous year and

161 May of the current year at Metheostation 7 (MP7) (Fig. 4b). In addition, we revealed a slight negative correlation with
162 precipitation in February-March of the current year.

163 As for the correlation between temperature and *P. koraiensis* growth, the analysis reveals a weak positive correlation
164 with the average monthly temperature in June of the previous year and in February-April of the current year in the
165 Chuguevka settlement and a slight negative correlation with the average monthly temperature in June-July as well
166 (Fig. 4c). The analysis of the correlation with the average monthly temperature at Metheostation 7 (MP7) shows us a
167 weak positive correlation with temperature in August and December of the preceding year and a negative correlation
168 with temperature in July of the current year (Fig. 4d). In addition, we analyzed the correlation with minimum average
169 monthly temperatures at MP7 and Chuguevka. The revealed correlation with minimum temperature is reliable but
170 weak (Fig. 4e,f).

171 Moreover, based on the weak interaction that was revealed, we analyzed the correlation with climatic parameters for
172 selected ranges of months (Fig. 4h,g). The most stable correlation appears between growth and the minimum monthly
173 temperature of August-December of the previous year at Chuguevka (Fig. 4h), on which we base our subsequent
174 reconstructions.

175 3.2 Minimum temperature reconstruction

176 Basing on analysis of the correlation between climatic parameters and Korean pine growth, we constructed a linear
177 regression equation to reconstruct the minimum monthly temperature of August-December of the previous year
178 (VUSr). The transfer function was as follows:

$$179 \text{VUSr} = 7.189X_t - 15.161$$

$$180 (N=32, R=0.620, R^2=0.385, R^2_{\text{adj}}=0.364, F=18.76, p < 0.001)$$

181 where VUSr is the August-December minimum temperature at Chuguevka and X is the tree-ring index of the Korean
182 pine RSC chronology in year t . The comparison between the reconstructed and observed mean growing season
183 temperatures during the calibration period is shown in Fig. 5(a). The cross-validation test for the calibration period
184 (1971-1997, $R=0.624$) yielded a positive RE of 0.334, a CE of 0.284, and the cross-validation test for calibration
185 period 1977-2003 ($R=0.542$) a positive RE of 0.654, a CE of 0.644, confirming the predictive ability of the model.

186 Although during the study period, the model shows the observed values very well, the short observation period (1971-
187 2003) does not allow using split-sampling calibration and verification methods in full for evaluating quality and model
188 stability. This limitation is why we used a bootstrapping resampling approach (Efron, 1979; Young, 1994) for stability
189 evaluation and transfer function precision. The idea that this method is based on indicates that the available data
190 already include all the necessary information for describing the empirical probability for all statistics of interest.
191 Bootstrapping can provide the standard errors of statistical estimators even when no theory exists (Lui et al., 2009).
192 The calibration and verification statistics are shown in Table 2. The statistical parameters used in bootstrapping are
193 very similar to those from the original regression model, and this proves that the model is quite stable and reliable and
194 that it can be used for temperature reconstruction.

195

196 3.3 Temperature variations from AD 1529 to 2014 and temperature periodicity

197 Variations in the reconstructed average minimum temperature of the previous August-December (VUSr) since AD
198 1529 and its 21-year moving average are shown in Fig. 5b. The 21-year moving average of the reconstructed series
199 was used to obtain low-frequency information and analyze temperature variability in this region. The mean value of

200 the 486-year reconstructed temperature was -7.93°C with a standard deviation of $\pm 1.40^{\circ}\text{C}$. We defined warm and
201 cold periods as when temperature deviated from the mean value plus or minus 0.5 times the standard deviation,
202 respectively (Fig. 5b).

203 Hence, warm periods occurred in 1561-1584, 1603-1607, 1614-1618, 1738-1743, 1756-1759, 1776-1781, 1944-2014,
204 and cold periods appeared in 1538-1543, 1549-1554, 1643-1649, 1659-1667, 1675-1689, 1722-1735, 1791-1803,
205 1807-1818, 1822-1827, 1836-1852, 1868-1887, 1911-1925. Among them, the four warmest years were in 1574 ($-$
206 4.35°C), 1606 (-5.35°C), 1615 (-5.71°C), 1741 (-5.36°C), 1757 (-6.16°C), 1779 (-5.21°C), 2008 (-2.72°C), while
207 the three coldest year were in 1543 (-9.84°C), 1551 (-9.88°C), 1647 (-10.77°C), 1662 (-11.10°C), 1685 (-9.45°C),
208 1728 (-10.08°C), 1799 (-10.70°C), 1815 (-10.13°C), 1825 (-9.87°C), 1843 (-10.55°C), 1883 (-10.73°C), 1913 ($-$
209 10.29°C). The longest cold period extended from 1868 to 1887, and the longest warm period extended from 1944 to
210 present day. The coldest year is 1662 (-11.10°C) and the warmest year is 2008 (-2.72°C).

211 The MTM spectral analysis over the full length of our reconstruction revealed significant ($p < 0.05$) cycle peaks at
212 2.3-year (95%), 2.5-year (99%), 2.9-year (99%), 3.0-year (99%), 3.3-year (95%), 3.7-year (95%), 8.9-year (99%)
213 short periods and 20.4-year (95%), 47.6-year (95%), 188.7-year (99%) long periods (Fig. 6).

214 Spatial correlations between our reconstruction and the CRU TS4.00 temperature dataset reveal our record's
215 geographical representation (Fig. 7). The results show that the reconstruction of mean minimum temperature of
216 previous August – December is significantly positively correlated with the CRU TS4.00 ($r=0.568$, $p<0.0001$).

217 4 Discussion

218 4.1 Climate-growth relationships

219 The results of our analysis suggest that the radial growth of Korean pine in the southern part of the Sikhote-Alin
220 mountain range is mainly limited by the pre-growth autumn-winter season temperatures, in particular the minimum
221 temperatures of August-December (Fig. 4). It is widely known that tree-ring growth in cold and wet ecotopes, situated
222 on sufficiently high elevation in the Northern Hemisphere, strongly correlate with temperature variability in large
223 areas of Asia, Eurasia, North America (Zhu et al., 2009; Anchukaitis et al., 2013; Thapa et al., 2015; Wiles et al.,
224 2014). The limiting influence of temperature on *P. koraiensis* growth has been mentioned in many studies (Wang et
225 al., 2016; Yin et al., 2009; Wang et al., 2013; Zhu et al., 2009). However, the temperature has various limiting effects
226 in different conditions, and these limiting effects manifest in different ways (Wang et al., 2016). For example, Zhu et
227 al., 2016 indicates that in more northern and arid conditions of the Zhangguangcai Mountains, while precipitation is
228 not the main limiting factor, precipitation is considerably below evaporation during the growth season. This finding
229 is why a stable correlation between *P. koraiensis* growth and the growth season temperature is revealed. This finding
230 is also why moisture availability in soil might be the main limiting factor for Korean pine growth (Zhu et al., 2016),
231 but the emergence of this circumstance can be different in different conditions.

232 The correlation between growth and minimum temperatures in August-December of the previous year, as revealed
233 in our research, was also mentioned for Korean pine in other works (Wang et al., 2016; Zhang et al., 2015). This
234 finding may be explained by the following circumstances. Extreme temperatures limit the growth of trees at the tree
235 line or in high-latitude forests (Wilson and Luckman, 2002; Körner and Paulsen, 2004; Porter et al., 2013; Yin et al.,
236 2015). Taking into consideration the fact that the study area is situated at the altitudinal limit of Korean pine forest
237 distributions, in particular the Korean pine (Kolesnikov, 1956), these findings seem to be reliable.

238 In addition, in the conditions close to extreme for this species, low temperatures in autumn-winter may lead to thicker
239 snow cover, which melts far more slowly in spring (Zhang et al., 2015). The study area is notable for its dry spring,
240 and the amount of precipitation is minimal during the most important period of tree-growth in April-May
241 (Kozhevnikova, 2009). If the vegetation period of the plant cannot begin at the end of March and packed snow cover
242 melting is impeded up until the beginning of May, plant growth may be reduced. Moreover, although cambial activity
243 stops in the winter, organic components are still synthesized by photosynthesis. Low temperatures (in the territory of
244 the VUSr it can reach -48°C in certain years) may induce to loss of accumulated materials, which adversely affects
245 growth (Zhang et al., 2015). The study area is in the center of the vegetated area, where the conditions for Korean
246 pine growth are optimal during the growing season, and only minimum temperature is regarded as an extreme factor.

247 4.2 Comparison with other tree-ring-based temperature reconstructions

248 At present, temperature reconstructions are uncommon for the Russian Far East, and research sites are located for
249 thousands of kilometers away from one another. For example, Wiles et al. undertook a study of summer temperatures
250 on Sakhalin Island (Wiles et al., 2014). Unfortunately, it is impossible to compare our findings with theirs because
251 Sakhalin Island is climatically far more similar to Japanese islands than to the Sikhote-Alin mountains, and
252 temperature variations in their study area are mainly caused by oceanic currents.

253 In addition, instrumental observations from the study area rarely encompass a period longer than 50 years (and studies
254 have only been conducted for large settlements). Consequently, the tree-ring record serves as a good indicator of the
255 past cold-warm fluctuations in the Russian Far East. The analysis of spatial correlations between our reconstruction
256 and the CRU TS4.00 temperature dataset reveal spatial correlations between the observed and reconstruction
257 minimum temperatures from the CRU TS4.00 gridded T_{\min} dataset during the baseline period of 1960-2003 (Fig. 7).
258 It's indicating that our temperature reconstruction is representative of large-scale regional temperature variations and
259 can be taken as representative of southeastern of the Russian Far East and northeastern of the China.

260 To identify the regional representativeness of our reconstruction, we compared it with two temperature reconstructions
261 for surroundings areas and a reconstruction for the Northern Hemisphere (Fig. 8). The first reconstruction was for
262 summer temperatures in the Northern Hemisphere (Wilson et al., 2016). The second reconstruction was an April-July
263 tree-ring-based minimum temperature reconstruction for Laobai Mountain (northeast China), which is approximately
264 500 km northwest of our site. The third was a February-April temperature reconstruction for the Changbai Mountain
265 (Zhu et al., 2009), which are approximately 430 km southwest of our site. Although the spring and summer
266 temperatures have been reconstructed in the last two cases, we use these reconstructions for comparison, because,
267 firstly, there are no other reconstructions for this region, and secondly, despite the possible seasonal shifts, long cold
268 and warm periods should be identified in all seasons.

269 Cold and warm periods are shown in table 3 (the duration is given by the authors of the article). The reconstructions
270 show that practically all cold and warm periods coincide but have different durations and intensities. The data on
271 Northern Hemisphere show considerable overlaps of cold and warm periods, and the correlation between
272 reconstructions is 0.45 ($p > 0.001$). At the same time, we found the warm period 1561-1584, which is not clearly
273 shown in reconstruction for the Northern Hemisphere, though the general trend of temperature change is maintained
274 during this period (Fig. 8). Long cold periods from 1643 to 1667 and 1675-1690 that were revealed for another territory
275 (Lyu et al., 2016; Wilson et al., 2016) coincided with the Maunder Minimum (1645-1715), an interval of decreased
276 solar irradiance (Bard et al., 2000). The coldest year in this study (1662) revealed in this period too. The Dalton
277 minimum period centered in 1810 is also notable. Interestingly that cold periods of 1807-1818, 1822-1827, 1836-1852
278 and 1868-1887 is also registered in reconstructions for Asia (Ohayama et al., 2013) and by Japanese researchers

279 (Fukaishi & Tagami, 1992; Hirano & Mikami, 2007). Moreover, instrumental observations reconstructed for western
280 Japanese territories (the nearest to the study area) provide evidence of a cold period in the 1830s-1880s with a short
281 warm spell in the 1850s (Zaiki et al., 2006), which is in agreement with our data (not reliably period 1855-1865, Tabl.
282 3). For this period, there are contemporaneous records of severe hunger in Japan in 1832 and 1839, which was the
283 result of a summer temperature decrease and rice crop failure (Nishimura & Yoshikawa, 1936).

284 In this case, the longer cold period for the study area can be explained by the relatively lower influence of the warm
285 current and monsoon and generally colder climate in the south of the Russian Far East compared with Japanese islands.
286 The differing opinion about the three cold periods in China in the 17th, 18th and 19th centuries (Wang et al., 2003) is
287 also corroborated by our reconstruction. The cold period in the 19th century is even more pronounced than that reported
288 by Lyu et al., 2016. Moreover, Lyu et al., 2016 corroborate that the ascertained cold period in 19th century is more
289 evident in South China, but it is less clear in the northern territories or has inverse trend. Although the Russian Far
290 East is further north than the southern Chinese provinces and is closer to the northern part of the country, the marked
291 monsoon climate likely made it possible to reflect the general cold trend in 19th century, which was typical both for
292 China and the entire Northern Hemisphere. Because of this possible explanation, the cold period in the 19th century
293 for the Changbai Mountains shows up more distinctly than for the northern and western territory of Laobai Mountain
294 (Fig. 8).

295 Apparently, this discrepancy in regional climate flow is the reason that our reconstruction agrees well with the general
296 reconstruction for the whole hemisphere ($r = 0.45, p < 0.001$) and to a lesser extent agrees with the regional curves for
297 Laobai Mountain ($r = 0.23, p < 0.001$) and Changbai Mountain ($r = 0.32, p < 0.001$).

298 The changing dynamics of the 20th century temperature is also interesting to watch. **The comparison of the minimum
299 annual temperatures for the territory and the reconstructed data for the period of 1960-2003 shows significant data
300 correlation (Fig. 7), including the northeast part of China.** At the same time, for Chinese territory (both for southwest
301 regions and for more northwestern regions), the warming is apparent only in the last quarter century (Zhu et al., 2009)
302 or at the end of the 20th century (Lyu et al., 2016) (Fig. 8 c,d). This trend, revealed for the southern Sikhote-Alin
303 mountains (a warm spell since 1944), is corroborated for the whole Northern Hemisphere (Wison et al., 2016) (Fig.
304 8a,b). The maximum cold period is also corroborated, which we note for the 19th century (Fig. 8a,b).

305 The probable explanation is in the regional climate flow differences in the compared data. The territory of northeastern
306 China is more continental, though the influence of the Pacific Ocean is also notable. At the same time, the southern
307 part of the Sikhote-Alin mountains is more prone to the influence of monsoons, as are the Japanese islands. According
308 to paleoreconstructions, the Little Ice Age occurred in the Northern Hemisphere 600-150 years ago (Borisova, 2014).
309 The period of landscape formation for the Sikhote-Alin range during the transition from the Little Ice Age to
310 contemporary conditions occurred within the last 230 years (Razzhigaeva et al., 2016). The timeframe of the Little
311 Ice Age is generally recognized as varying considerably depending on the region (Bazarova et al., 2014). However, it
312 is certain that the Little Ice Age is accompanied by an increase in humidity in coastal areas of northeast Asia (Bazarova
313 et al., 2014). Thus, in similar conditions on the Japanese islands, the Little Ice Age was accompanied by lingering and
314 intensive rains (Sakaguchi, 1983), and the last typhoon activity was registered for the Japanese islands from the middle
315 of the 17th century to the end of the 19th century (Woodruff et al., 2009). At the same time, the reconstruction of
316 climatic changes for the whole territory of China for the last 2000 years (Ge et al., 2016) shows that the cold period
317 lasted until 1920, which correlates with the data we obtained. This timespan wholly coincides with our data, and we
318 can draw the conclusion that in the southern region of the Sikhote-Alin mountains, the Little Ice Age ended at the turn
319 of the 19th century.

320 Unfortunately, when comparing temperature, different changes were also observed for some cold and warm years
321 (Fig. 8). This finding may be attributed to differences in the reconstructed temperature parameters (such as average
322 value, minimum temperature and maximum temperature) and environmental conditions in different sampling regions.
323 Recent studies show that the oscillations in the medium, minimum and maximum temperature are often asymmetrical
324 (Karl et al., 1993; Xie and Cao, 1996; Wilson and Luckman, 2002, 2003; Gou et al., 2008). The global warming over
325 the past few decades has been mainly caused by the rapid growth of night or minimum temperatures but not maximum
326 temperatures. Meanwhile, some differences between the reconstructed temperature values were well explained by a
327 comparison with similar areas.

328 We can conclude that the analysis shows that the reconstructed data is representative for large-scale regional
329 temperature variations (Fig. 7). At the same time, some cold and warm periods in our reconstruction and other
330 neighbored studies do not coincide (Fig. 8), which can be due to the reconstruction of other climatic parameters and
331 differing environmental conditions. So, we believe that these results can characterize regional climate variations and
332 provide reliable data for large-scale reconstructions for the northeastern portion of Eurasia, but their use for large-
333 scale regional reconstructions requires further research.

334 4.3 Periodicity of climatic changes and their links to global climate processes

335 Among the significant periodicities in the reconstructed temperature detected by the MTM analysis (Fig. 7), some
336 peaks were singled out: 2.3-year (95%), 2.5-year (99%), 2.9-year (99%), 3.0-year (99%), 3.3-year (95%), 3.7-year
337 (95%), 8.9-year (99%) short periods and 20.4-year (95%), 47.6-year (95%), and 188.7-year (99%) long periods.

338 The 2-4-year cycle may be linked with the El Niño-Southern Oscillation (ENSO). These high-frequency (2-7-year)
339 cycles (Bradley *et al.*, 1987) have also been found in other tree-ring-based temperature reconstructions in northeast
340 Asia (Zhu *et al.*, 2009; Li and Wang, 2013; Zhu et al., 2016; Gao et al., 2015).

341 The 2–3-year quasi-cycles may also correspond to the quasi-biennial oscillation (Labitzke and van Loon, 1999) and
342 the tropospheric biennial oscillation (Meehl, 1987), whereas the 8.9-11.5-year cycles may correspond to solar activity.
343 Considering the coincidence of these two episodes, the Maunder Minimum (1645–1715) and the Dalton minimum
344 period centered in 1810, the revealed periodicity seems reliable.

345 It seems that next low-frequency cycles of 20 and 48 years reflect processes influenced by Pacific Decadal Oscillation
346 (PDO, Mantua and Hare 2002) variability, which has been found at 15-25-yr and 50-70-yr cycles (Ma, 2007).

347 Given that many researchers working in the territory of northeast Asia have also revealed these cycles in relation to
348 the Korean pine, we can draw a conclusion that Korean pine tree-ring series support the concept of long-term,
349 multidecadal variations in the Pacific (e.g., D'Arrigo et al., 2001; Cook, 2002) and that such variation or shifts have
350 been present in the Pacific for several centuries.

351 Despite the fact that it is quite difficult to reveal for certain long-period cycles in a 486-year chronology, we
352 nonetheless revealed the 189-year cycle. Such periodicity is revealed in long-term climate reconstructions and is
353 linked to the quasi-200-year solar activity cycle (Raspopov et al., 2009). Such climate cycling, linked not only to
354 temperature but also to precipitation, is revealed for the territories of Asia, North America, Australia, Arctic and
355 Antarctic (Raspopov et al., 2008). At the same time, the 200-year cycle (*de-Vries* cycle) may often have a phase shift
356 from some years to decades and correlates not only positively but also negatively with climatic fluctuations depending
357 on the character of the nonlinear response of the atmosphere-ocean system within the scope of the region (Raspopov
358 et al., 2009). According to Raspopov et al. (2009), the study area is in the zone that reacts with a positive correlation
359 to solar activity, though the authors note that we should not expect a direct response because of the nonlinear character
360 of the atmosphere-ocean system reaction to variability in solar activity (Raspopov et al., 2009). Taking into

361 consideration this fact and that the cold and warm periods shown in our reconstruction are slightly shifted compared
362 with more continental areas and the whole Northern Hemisphere, we can say that the reconstruction of minimum
363 August-December temperatures reflects the global climate change process in aggregate with the regional
364 characteristics of the study area.

365 **Conclusions**

366 Using the tree-ring width of *Pinus koraiensis*, the mean minimum temperature of the previous August-December has
367 been reconstructed for the southern part of Sikhote-Alin Mountain Range, northeastern Asia, Russia, for the past 486
368 years. This dataset is the first climate reconstruction for this region, and for the first time for northeast Asia, we present
369 a reconstruction with a length exceeding 486 years.

370 Because explained variance of our reconstruction is about 39%, we believe that the result is noteworthy as it displays
371 the respective temperature fluctuations for the whole region, including northeast China, the Korean peninsula and the
372 Japanese archipelago. Our reconstruction is also in good agreement with the climatic reconstruction for the whole
373 Northern Hemisphere. The reconstruction shows good agreement with the cold periods described by documentary
374 notes in eastern China and Japan. All these comparisons prove that for this region, the climatic reconstruction based
375 on tree-ring chronology has a good potential to provide a proxy record for long-term, large-scale past temperature
376 patterns for northeast Asia. The results display the cold and warm periods in the region, which are conditional on
377 global climatic processes (PDO, ENSO), and reflect the influence of solar activity (we revealed the influence of the
378 11-year and 200-year solar activity cycles). At the same time, the reconstruction highlights the peculiarities of the
379 flows of global process in the study area and helps in understanding the processes in the southern territory of the
380 Russian Far East for more than the past 450 years. Undoubtedly, the results of our research are important for studying
381 the climatic processes that have occurred in the study region and in all of northeastern Asia and for situating them
382 within the scope of global climatic change.

383

384 **Acknowledgements** This work was funded by Russian Foundation for Basic Research, Project 15-04-02185.

385 **References**

- 386 Anchukaitis K.J., D'Arrigo R.D., Andreu-Hayles L., Frank D., Verstege A., Curtis A., Buckley B.M., Jacoby G.C.,
387 and Cook E.R.: Tree-ring-reconstructed summer temperatures from Northwestern North America during the last
388 nine centuries. *J Clim.* 26, 3001-3012, doi: 10.1175/JCLI-D-11-00139.1, 2013.
- 389 Bard E., Raisbeck G., Yiou F. and Jouzel J.: Solar irradiance during the last 1200 years based on cosmogenic
390 nuclides. *Tellus B.*, 52, 985-992, 2000.
- 391 Bazarova V.B., Grebennikova T.A., and Orlova L.A.: Natural-environment dynamic within the Amur basin during
392 the neoglacial. *Geogr. Nat. Resour.*, 35(3), 275-283, doi: 10.1134/S1875372814030111, 2014.
- 393 Bond G., Kromer B., Beer J., Muscheler R., Evans M.N., Showers W., Hoffmann S., Lotti-Bond R., Hajdas I.,
394 Bonani G.: Persistent solar influence on north Atlantic climate during the Holocene. *Sci.*, 294, 2130–2136, 2001.
- 395 Borisova O.K.: Landscape-climatic changes in Holocene. *Reg. Res. Rus.*, 2, 5-20, 2014.
- 396 Bradley R.S., Diaz H.F., Kiladis G.N., Eischeid J.K.: ENSO signal in continental temperature and precipitation
397 records. *Nat.* 327, 497-501, 1987.

398 Cook E.R., Kairiukstis L.A.: Methods of dendrochronology: applications in the environmental sciences. Kluwer
399 Academic Publishers, Dordrecht, 1990.

400 Cook E.R.: Reconstructions of Pacific decadal variability from long tree-ring records. Eos Trans. 83 (19) Spring
401 Meet. Suppl., Abstract GC42A-04, 2002.

402 Corona C., Guiot J., Edouard J.L., Chalié F., Büntgen U., Nola P. and Urbinati C.: Millennium-long summer
403 temperature variations in the European Alps as reconstructed from tree rings. Clim. Past., 6, 379-400,
404 doi:10.5194/cp-6-379-2010, 2012.

405 Dai L.M., Qi L., Su D.K., Wang Q.W., Ye Y.J. and Wang Y.: Changes in forest structure and composition on
406 Changbai Mountain in Northeast China. Ann. For. Sci., 68, 889-897, 2011.

407 Ding Y., Dai X.: Temperature Variation in China during the Last 100 years. Meteorology, 20, 19-26, 1994.

408 Durbin J. and Watson G.S.: Testing for serial correlation in least squares regression. Biometrika, 38, 159-178, 1951.

409 Efron B.: The jackknife, the bootstrap, and other resampling plans. Pa. Soc. for Industrial and Appl. Mathem.,
410 Philadelphia, 1982.

411 Efron B.: Bootstrap methods: another look at the jackknife. Annals Statistics, 7, 1-26, 1979.

412 Fritts H.C.: Tree rings and climate. Academic Press Inc., London, 1976.

413 Fukaishi K. and Tagami Y.: An attempt of reconstructing the winter weather situations from 1720–1869 by the use
414 of historical documents. In: Proceedings of the International Symposium on the Little Ice Age Climate, Department
415 of Geography, Tokyo Metropolitan University, Tokyo, 194-201, 1992.

416 Ge Q., Zheng J., Hao Z., Liu Y. and Li M.: Recent advances on reconstruction of climate and extreme events in
417 China for the past 2000 years. J Geogr Sci 26(7), 827-854, doi: 10.1007/s11442-016-1301-4, 2016.

418 Gou X., Chen F., Yang M., Gordon J., Fang K., Tian Q. and Zhang Y.: Asymmetric variability between maximum
419 and minimum temperatures in Northeastern Tibetan Plateau: evidence from tree rings. Sci. China. Ser. D. 51, 41-55,
420 2008.

421 Hirano J. and Mikami T.: Reconstruction of winter climate variations during the 19th century in Japan. Int J
422 Climatol 28, 1423-1434, doi:10.1002/joc.1632, 2007.

423 Holmes R.L.: Computer-assisted quality control in tree-ring dating and measurement. Tree-ring Bull. 43, 69-78,
424 1983.

425 Ishikawa Y., Krestov P.V. and Namikawa K.: Disturbance history and tree establishment in old-growth *Pinus*
426 *koraicensis*-hardwood forests in the Russian Far East. J. Veg. Sci. 10, 439-448, 1999.

427 Karl T.R., Jones P.D., Knight R.W., Kulas G., Plummer N., Razuvayev V., Gallo K.P., Lindsey J., Charlson R.J.,
428 and Peterson T.C.: A new perspective on recent global warming: asymmetric trends of daily maximum and
429 minimum temperature. B. Am. Meteorol. Soc., 74, 1007-1023, 1993.

430 Kolesnikov B.P.: Korean pine forests of the [Russian] Far East. Trudy DVF AN SSSR. 2, 1-264, 1956 (In Russian).

431 Körner C. and Paulsen J.: A world-wide study of high altitude treeline temperatures. J. Biogeogr., 31, 713-732,
432 doi:10.1111/j.1365-2699.2003.01043.x, 2004.

433 Kozhevnikova N.K.: Dynamics of weather-climatic characteristics and ecological function of small river basin. Sib.
434 Ecol. J., 5, 93-703, 2009 (In Russian).

435 Kress A., Hangartner S., Bugmann H., Büntgen U., Frank D.C., Leuenberger M., Siegwolf R.T.W. and Saurer M.:
436 Swiss tree rings reveal warm and wet summers during medieval times. Geophys. Res. Lett., 41, 1732-1737, doi:
437 10.1002/2013GL059081, 2014.

438 Labitzke K.G. and van Loon H.: The Stratosphere: Phenomena, History and Relevance. Springer, Berlin, 1999.

439 Lean J. and Rind D.: Evaluating sun-climate relationships since the Little Ice Age. *J. Atmos. Sol. Terr. Phys.*, 61,
440 25-36, 1999.

441 Li M. and Wang X.: Climate-growth relationships of three hard- wood species and Korean pine and minimum
442 temperature reconstruction in growing season in Dunhua, China. *J. Nanjing. For. Univ.*, 37, 29-34, 2013.

443 Liu Y., Bao G., Song H., Cai Q. and Sun J.: Precipitation reconstruction from Hailar pine (*Pinus koraiensis* var.
444 *mongolica*) tree rings in the Hailar region, Inner Mongolia, China back to 1865 AD. *Paleogeogr Paleoclimatol*
445 *Paleoecol*, 282, 81-87, doi:10.1016/j.palaeo.2009.08.012, 2009.

446 Liu Q.J.: Structure and dynamics of the subalpine coniferous forest on Changbai mountain, China. *Plant. Ecol.* 132,
447 97-105, 1997.

448 Lu R., Jia F., Gao S., Shang Y. and Chen Y.: Tree-ring reconstruction of January-March minimum temperatures
449 since 1804 on Hasi Mountain, northwestern China. *J. Arid. Environ.*, 127, 66-73,
450 doi:10.1016/j.jaridenv.2015.10.020, 2016.

451 Lyu S., Li Z., Zhang Y. and Wang X.: A 414-year tree-ring-based April–July minimum temperature reconstruction
452 and its implications for the extreme climate events, northeast China. *Clim. Past.* 12, 1879-1888, doi:10.5194/cp-12-
453 1879-2016, 2016.

454 Ma Z.G.: The interdecadal trend and shift of dry/wet over the central part of north China and their relationship to the
455 Pacific Decadal Oscillation (PDO). *Chin. Sci. Bull.*, 52(12), 2130-2139, 2007.

456 Mantua N., Hare S.: The Pacific decadal oscillation. *J. Oceanogr.* 58(1), 35-44, 2002.

457 Meehl G.A.: The annual cycle and interannual variability in the tropical Pacific and Indian Ocean regions. *Mon.*
458 *Weather. Rev.*, 115, 27-50, 1987.

459 Melvin T.M. and Briffa K.R.: A ‘signal-free’ approach to dendroclimatic standardisation. *Dendrochronologia*, 26,
460 71-86, doi: 10.1016/j.dendro.2007.12.001, 2008.

461 Nishimura M. and Yoshikawa I.: Nippon Kyokoshi Ko, Maruzen, Tokyo, an archival collection of disasters in
462 Japan, 1936 (in Japanese)

463 Ohayama M., Yonenobu H., Choi J.N., Park W.K., Hanzawa M. and Suzuki M.: Reconstruction of northeast Asia
464 spring temperature 1784-1990. *Clim. Past.*, 9, 261-266, doi:10.5194/cp-9-261-2013, 2013.

465 Omelko A., Ukhvatkina O. and Zmerenetsky A.: Disturbance history and natural regeneration of an old-growth
466 Korean pine-broadleaved forest in the Sikhote-Alin mountain range, Southeastern Russia. *For. Ecol. Manag.* 360,
467 221-234, doi: 10.1016/j.foreco.2015.10.036, 2016.

468 Omelko A.M. and Ukhvatkina, O.N.: Characteristics of gap-dynamics of conifer-broadleaved forest of Southen
469 Sikhote-Alin (Russia). *Plant World Asian Russ.*, 1, 106-113, 2012.

470 Popa I. and Bouriaud O.: Reconstruction of summer temperatures in Eastern Carpathian Mountain (Rodna Mts,
471 Romania) back to AD 1460 from tree-rings. *Int. J. Climatol.*, 34, 871-880, doi: 10.1002/joc.3730, 2014.

472 Porter T.J., Pisaric M.F., Kokelj S.V. and DeMontigny P.: A ring-width-based reconstruction of June-July minimum
473 temperatures since AD 1245 from white spruce stands in the Mackenzie Delta region, northwestern Canada.
474 *Quaternary. Res.*, 80, 167-179, doi: 10.1016/j.yqres.2013.05.004, 2013.

475 Raspopov OM, Dergachev VA, Esper J, Kozyreva OV, Frank D, Ogurtsov M, Kolström T, Shao X (2008) The
476 influence of the de Vries (~200-year) solar cycle on climate variations: Results from the Central Asian
477 Mountains and their global link. *Palaeogeogr Palaeoclimatol Palaeoecol* 259:6-16. doi:
478 10.1016/j.palaeo.2006.12.017

479 Raspopov O.M., Dergachev V.A., Kozyreva O.V., Kolström T., Lopatin E.V. and Luckman B.: Geography of 200-
480 year climate periodicity and Long-Term Variations of Solar activity. *Reg. Res. Russ.*, 2, 17-27, 2009.

481 Razzhigaeva N.G., Ganzei L.A., Mokhova L.M., Makarova T.R., Panichev A.M., Kudryavtseva E.P., Arslanov
482 Kh.A., Maksimov F.E. and Starikova A.A.: The Development of Landscapes of the Shkotovo Plateau of Sikhote-
483 Alin in the Late Holocene. *Reg. Res. Russ.*, 3, 65-80, doi:10.15356/0373-2444-2016-3-65-80, 2016.

484 Ren F. and Zhai P.: Study on Changes of China's Extreme Temperatures During 1951–1990. *Sci. Atmos. Sin.*, 22,
485 217-227, 1998.

486 Sakaguchi Y.: Warm and cold stages in the past 7600 years in Japan and their global correlation. *Bull. Dep. Geogr.*
487 15, 1-31, 1983.

488 Shao X. and Wu X.: Reconstruction of climate change on Changbai Mountain, Northeast China using tree-ring data.
489 *Quaternary. Sci.*, 1, 76-83, 1997.

490 Stokes M.A. and Smiley T.L.: *Tree-ring dating*. The University of Chicago Press, Chicago, London, 1968.

491 Tang H., Zhai P. and Wang Z.: On Change in Mean Maximum Temperature, Minimum Temperature and Diurnal
492 Range in China During 1951–2002. *Climatic Environ Res.*, 10, 728-735, 2005.

493 Thapa U.K., Shan S.K., Gaire N.P. and Bhujju D.R.: Spring temperatures in the far-western Nepal Himalaya since
494 1640 reconstructed from *Picea smithiana* tree-ring widths. *Clim dyn*, 45(7), 2069-2081, doi: 10.1007/s00382-014-
495 2457-1, 2015.

496 Wang H., Shao X.M., Jiang Y., Fang X.Q. and Wu S.W.: The impacts of climate change on the radial growth of
497 *Pinus koraiensis* along elevations of Changbai Mountain in northeastern China. *For. Ecol. Manag.*, 289, 333-340,
498 doi:10.1016/j.foreco.2012.10.023, 2013.

499 Wang X., Zhang M., Ji Y., Li Z., Li M. and Zhang Y.: Temperature signals in tree-ring width and divergent
500 growth of Korean pine response to recent climate warming in northeast Asia. *Trees* 31(2), 415-427, doi:
501 10.1007/s00468-015-1341-x, 2016.

502 Wang S., Liu J. and Zhou J.: The Climate of Little Ice Age Maximum in China. *J. Lake. Sci.*, 15, 369-379, 2003.

503 Wang W., Zhang J., Dai G., Wang X., Han S., Zhang H. and Wang Y.: Variation of autumn temperature over the
504 past 240 years in Changbai Mountain of Northeast China: A reconstruction with tree-ring records. *China. J. Ecol.*,
505 31, 787-793, 2012.

506 Wang Z., Ding Y., He J. and Yu J.: An updating analysis of the climate change in China in recent 50 years. *Ac*
507 *Meteorol Sin*, 62, 228-236, 2004.

508 Wigley T.M.L., Briffa K.R. and Jones P.D.: On the average value of correlated time series, with applications in
509 dendroclimatology and hydrometeorology. *J. Clim. Appl. Meteorol.*, 23, 201-213, 1984.

510 Wiles G.C., Solomina O., D'Arrigo R., Anchukaitis K.J., Gensiarovsky Y.V. and Wiesenberg N.: Reconstructed
511 summer temperatures over the last 400 year a based on larch ring widths: Sakhalin Island, Russian Far East. *Clim.*
512 *Dyn.*, 45, 397-405, doi: 10.1007/s00382-014-2209-2, 2014.

513 Wilson R.J.S. and Luckman B.H.: Tree-ring reconstruction of maximum and minimum temperatures and the diurnal
514 temperature range in British Columbia, Canada. *Dendrochronologia*, 20, 1-12, 2002.

515 Wilson R.J.S., Luckman B.H.: Dendroclimatic reconstruction of maximum summer temperatures from upper
516 treeline sites in Interior British Columbia, Canada. *Holocene*, 13, 851-861, doi:10.1191/0959683603hl663rp, 2003.

517 Xie Z. and Cao H.: Asymmetric changes in maximum and minimum temperature in Beijing. *Theor Appl Climatol*,
518 55, 151-156, 1996.

519 Yin H., Guo P., Liu H., Huang L., Yu H., Guo S. and Wang F.: Reconstruction of the October mean temperature
520 since 1796 at Wuying from tree ring data. *Adv. Clim. Change. Res.*, 5, 18-23, 2009.

521 Yin H., Liu H., Linderholm H.W. and Sun Y.: Tree ring density-based warm-season temperature reconstruction
522 since AD 1610 in the eastern Tibetan Plateau. *Palaeogeogr, Palaeoclimatol, Palaeoecol*, 426, 112-120, doi:
523 10.1016/j.palaeo.2015.03.003, 2015.

524 Young G.A.: Bootstrap: more than a stab in the dark. *Statistical. Sci.* 9, 382-415, 1994.

525 Zaiki M., Können G., Tsukahara T., Jones P., Mikami T. and Matsumoto K.: Recovery of nineteenth-century
526 Tokyo/Osaka meteorological data in Japan. *Int J Climatol*, 26, 399-423, doi:10.1002/joc.1253, 2006.

527 Zang C. and Biondi F.: Treeclim: an R package for the numerical calibration of proxy-climate relationships. *Ecogr.*
528 38, 001-006, doi: 10.1111/ecog.01335, 2015.

529 Zhang R.B., Yuan Y.J., Wei W.S., Gou X.H., Yu S.L., Shang H.M., Chen F., Zhang T.W. and Qin L.:
530 Dendroclimatic reconstruction of autumn-winter mean minimum temperature in the eastern Tibetan Plateau since
531 1600 AD. *Dendrochronologia*, 33, 1-7, doi: 10.1016/j.dendro.2014.09.001, 2015.

532 Zhao C., Ring G., Zhang Y., Wang Y.: Climate change of the Northeast China over the past 50 years. *J. Arid. Land.*
533 *Resour. Environ.*, 23, 25-30, 2009.

534 Zhu H.F., Fang X.Q., Shao X.M. and Yin Z.: Tree-ring-based February-April temperature reconstruction for
535 Changbai Mountain in Northeast China and its implication for East Asia winter monsoon. *Clim Past.*, 5, 661-666,
536 2009.

537 Zhu L., Li Z., Zhang Y. and Wang X.: A 211-year growing season temperature reconstruction using tree-ring width
538 in Zhangguangcai Mountains, Northeast China: linkages to the Pacific and Atlantic Oceans. *Int. J. Climatol.*, doi:
539 10.1002/joc.4906, 2016.

540 Zhu L., Li S., Wang X.: Tree-ring reconstruction of February-March mean minimum temperature back to 1790 AD
541 in Yichun, Northeast China. *Quaternary. Sci.*, 35, 1175-1184, doi: 10.11928/j.issn.1001-7410.2015.05.13, 2015.

542 **Tables and Figures**

543 **Table 1.** The sampling information and statistics of the signal-free chronology

	VUSr
Elevation (m a.s.l.)	700-900
Latitude (N), Longitude (E)	44°01'32'', E 134°13'15''
Core (live trees) / sample (dead trees)	25/20
Time period / length (year)	1451-2014 / 563
MS	0.253
SD	0.387
AC1	0.601
R	0.691
EPS	0.952
Period with EPS>0.85 / length (year)	1602-2014 / 412
Period with EPS>0.75 / length (year)	1529-2014 / 485
Skew/Kurtosis	0.982/5.204

544 MS – mean sensitivity, SD – standard deviation, AC1 – first-order autocorrelation, EPS – expressed population signal

545

546 **Table 2.** Calibration and verification statistics of the reconstruction equation for the common period 1971-2003 of

547 **Bootstrap**

Statistical item	Calibration	Verification (Bootstrap, 199 iterations)
r	0.62	0.62 (0.54-0.70)
R ²	0.39	0.39 (0.27-0.41)
R ² _{adj}	0.36	0.37 (0.37-0.40)
Standard error of estimate	1.20	1.11
F	18.76	18.54
P	0.0001	0.0001
Durbin-Watson	1.73	1.80

548

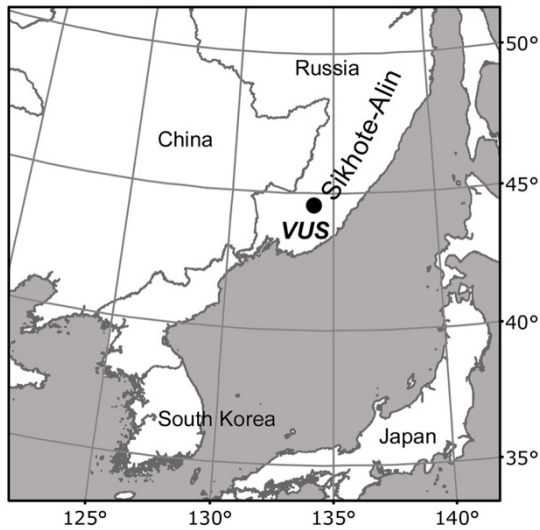
549 **Table 3.** Cold and warm periods based on the results of this study compared with other researches

Period	Southern Sikhote-Alin (this study)	Laobai Mountain (Lyu et al., 2016)	Changbai Mountain (Zhu et al., 2009)
Cold	1538-1544; 1549-1554	*	*
	—	1605-1616	
	1643-1649; 1659-1667	1645-1677	*
	1675-1689	1684-1691	*
	1791-1801; 1807-1818	—	1784-1815
	1822-1827; 1836-1852		1827-1851
	1868-1887	—	1878-1889
	1911-1925	1911-1924; 1930-1942; 1951-1969	1911-1945
Warm	1561-1584	*	*

1603-1607; 1614-1618	—	*
1738-1743	—	—
1756-1759; 1776-1781	1767-1785	1750-1783
<i>1787-1793**</i>	1787-1793	—
<i>1795-1807**</i>	1795-1807	—
<i>1855-1865**</i>	—	1855-1877
1944-2014	1991-2008	1969-2009

550 Note: *italic *** – the periods which agreement with VUSr but not reliably for VUSr; * - the reconstruction not
551 covering this period.

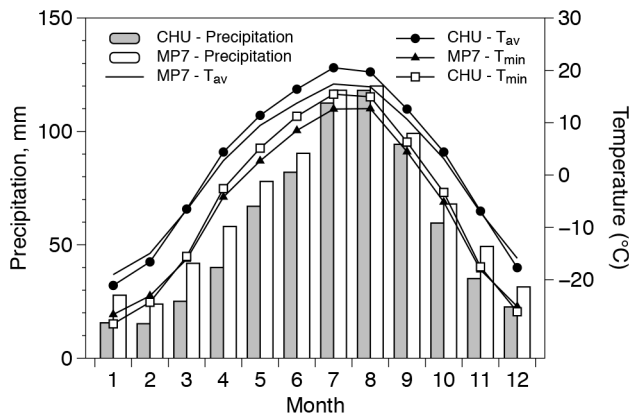
552



553

554 **Figure 1:** Location of the study area on the Sikhote-Alin Mountains, Southeastern Russia. VUS is Verkhneussyriysky

555 Research Station

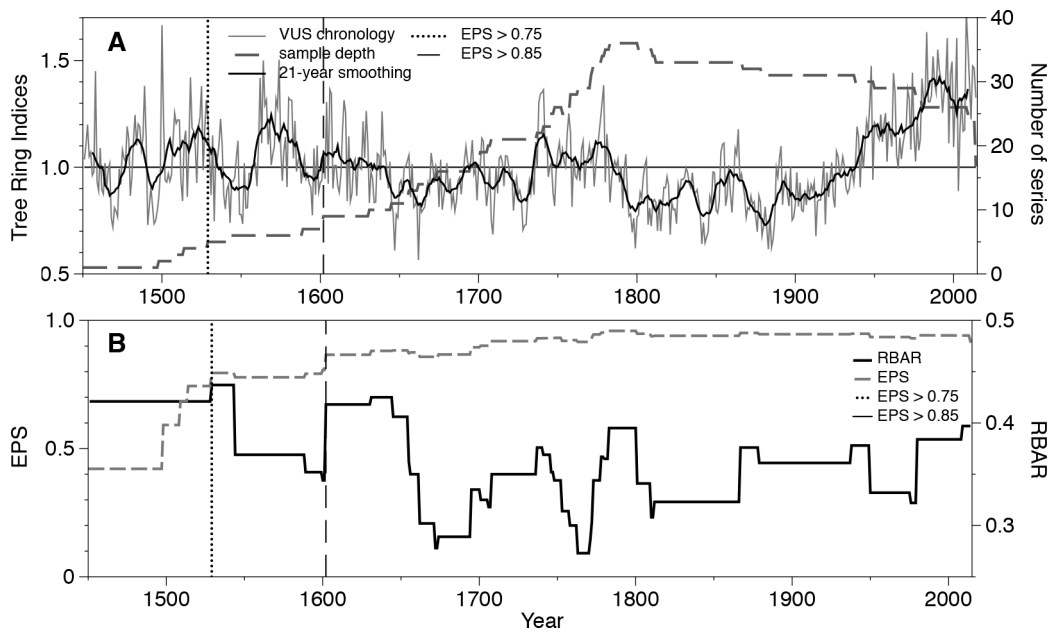


556

557 **Figure 2:** Mean monthly (1936-2004), minimum temperature (1971-2003) and total precipitation (1936-2004) at

558 Chuguevka and mean monthly, minimum temperature and total precipitation for VUS meteorological station (MP7)

559 (1966-2000)

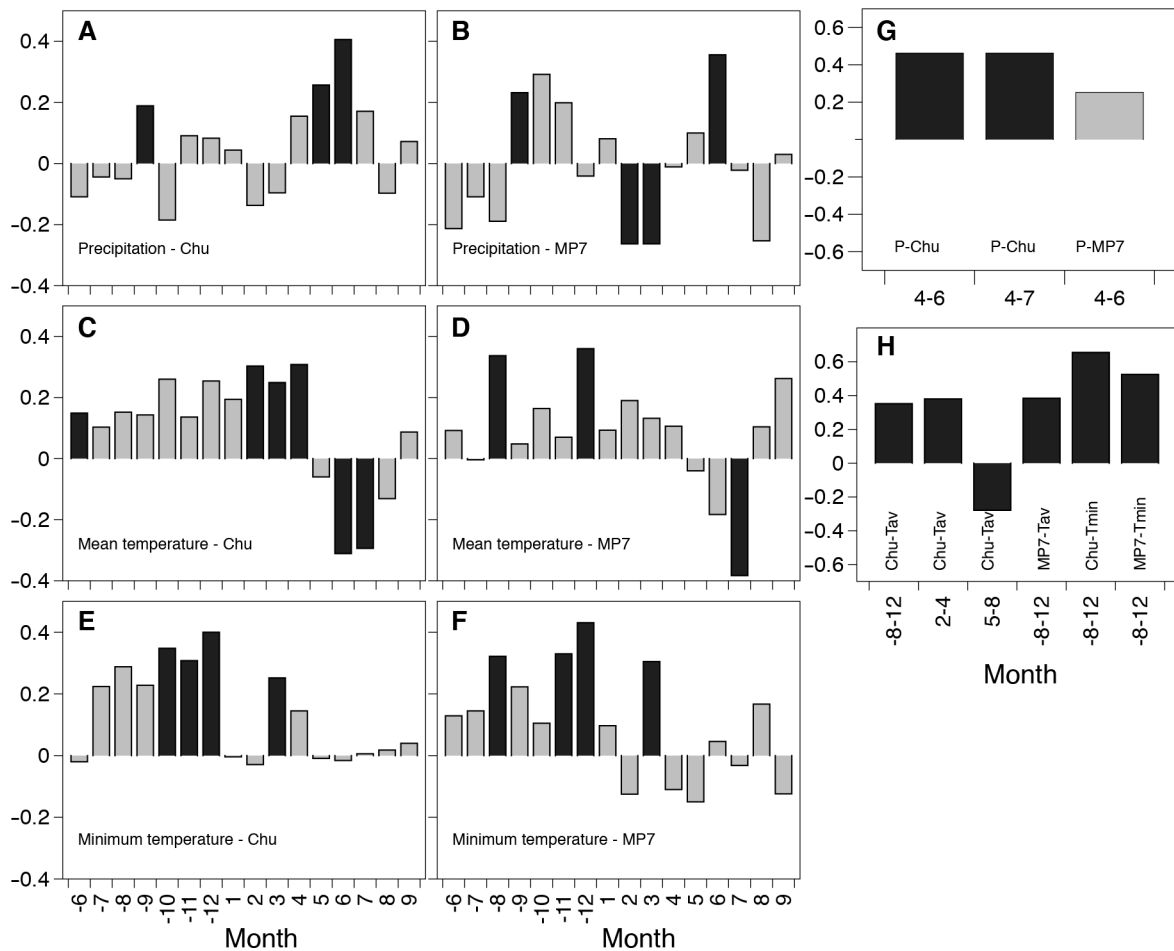


560

561

Figure 3: Variations of the VUS chronology and sample depth (a) and the expressed population signal (EPS) and average correlation between all series (Rbar) VUS chronology from AD 1451 to 2014 (b)

562



563

564

Figure 4: Correlations between the monthly mean meteorological data and VUS chronology

565

A, C, E – Chuguevka (Chu) and VUS chronology; B, D, F - VUS meteorological station (MP7) and VUS chronology;

566

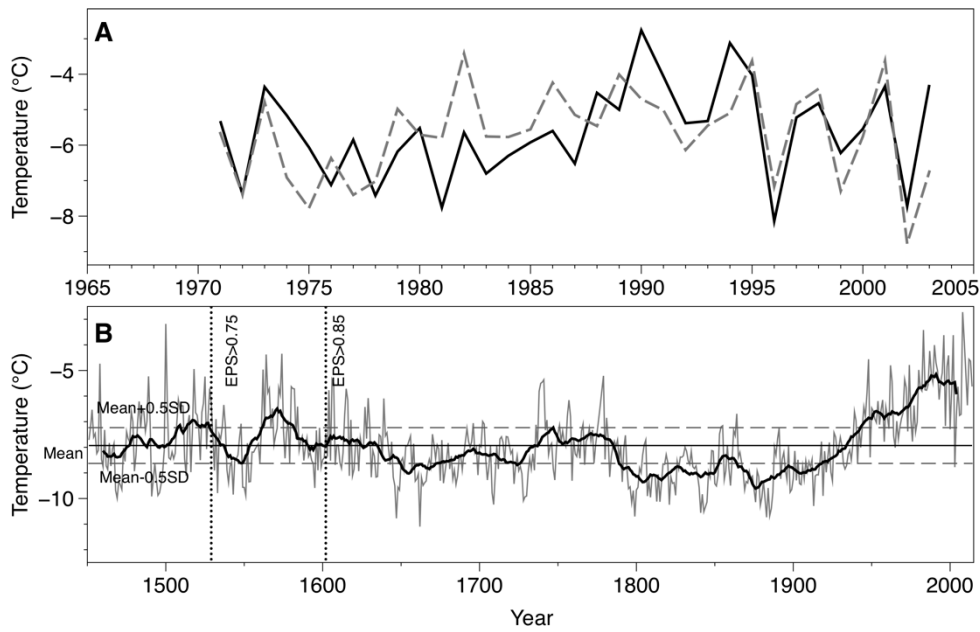
G – correlation coefficients between VUS chronology and the precipitation of different month combinations; H –

567

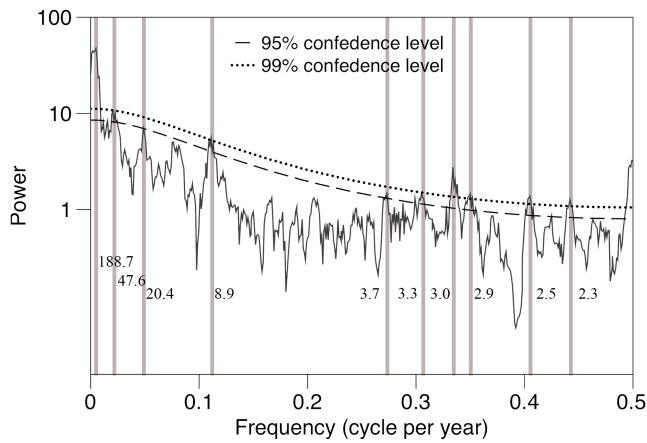
correlation coefficients between VUS chronology and the temperature of different month combinations. The black

568

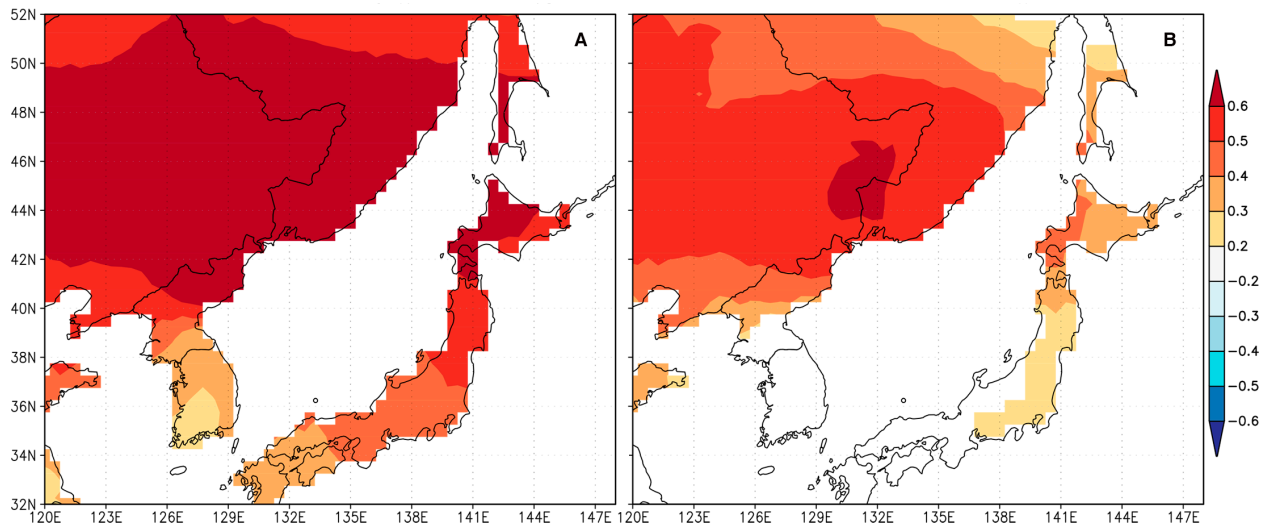
bars are significant value.



569
 570 **Figure 5:** (a) Actual (black line) and reconstructed (dash line) August – December minimum temperature for the
 571 common period of 1971-2003; (b) reconstruction of August – December minimum temperature (VUSr) to Southern
 572 part of Sikhote-Alin for the last 563 years. The smoothed line indicates the 21-year moving average.

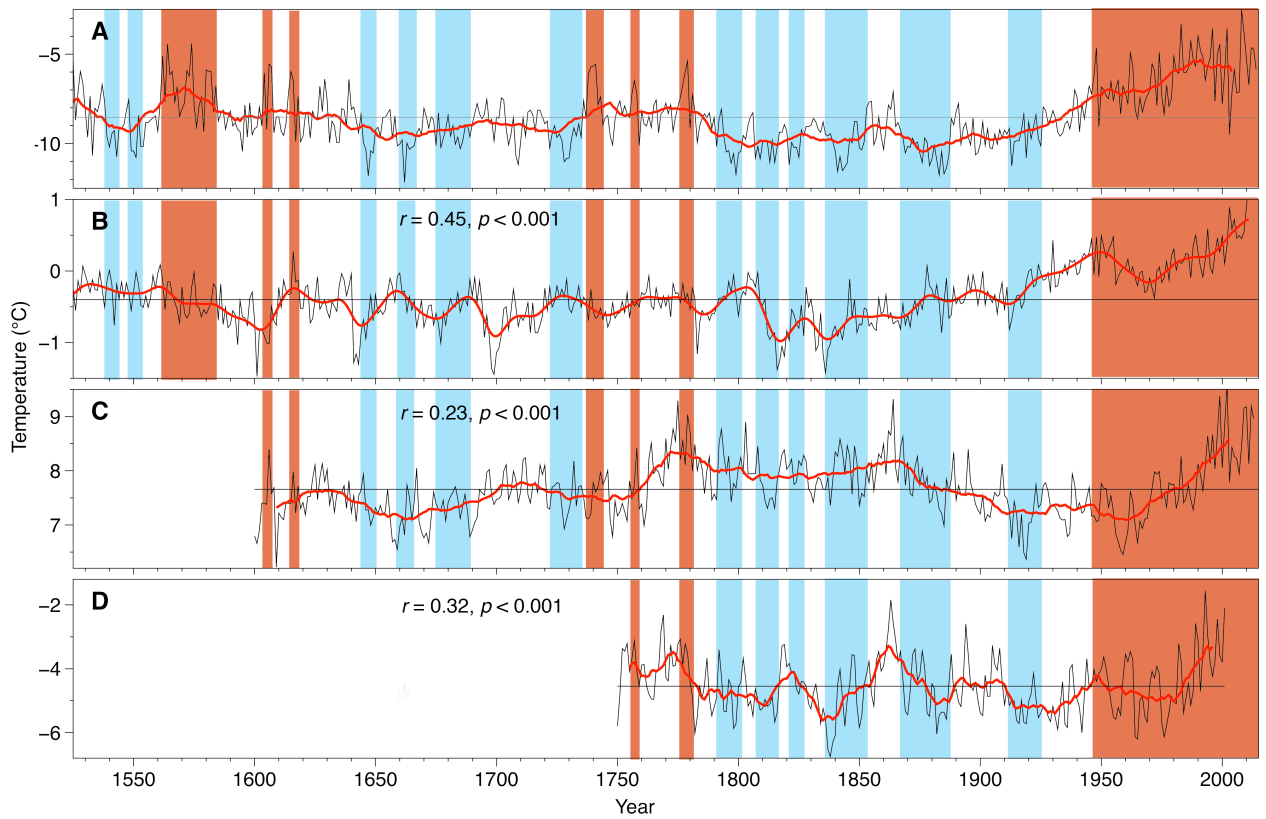


573
 574 **Figure 6:** The MTM power spectrum of the reconstructed August – December minimum temperature (VUSr) from
 575 1529 to 2014



576

577 **Figure 7:** Spatial correlations between the observed (a) and reconstructed (b) August – December minimum
 578 temperature (VUS) in this study and regional gridded annual minimum temperature from CRU TS 4.00 over their
 579 common period 1960–2003 ($p < 10\%$)
 580



581
 582 **Figure 8:** (a) August-December mean minimum temperature reconstructed (VUSr) on southern part of Sikhote-
 583 Alin, (b) Northern Hemisphere extratropical temperature (Willes et al., 2016), (c) April – July minimum temperature
 584 on Laobai Mountain by Lyu et al., 2016, and (d) February – April temperature established by Zhu et al. (2009) on
 585 Changbai Mountain. Black lines denote temperature reconstruction values, and red color lines indicate the 21-year
 586 moving average; red and blue fields – warm and cold period consequently (in this study)